

1 **Reduced-complexity air quality intervention modelling** 2 **over China: development of the InMAPv1.6.1-China and** 3 **comparison with the CMAQv5.2 model**

4 Ruili Wu¹, Christopher W. Tessum², Yang Zhang³, Chaopeng Hong⁴, Yixuan Zheng⁵,
5 Qiang Zhang¹

6 ¹Ministry of Education Key Laboratory for Earth System Modelling, Department of Earth System
7 Science, Tsinghua University, Beijing 100084, China

8 ²Department of Civil and Environmental Engineering, University of Illinois at Urbana-Champaign,
9 Urbana, Illinois 61801, United States

10 ³Department of Civil and Environmental Engineering, Northeastern University, Boston, Massachusetts
11 02115, United States

12 ⁴Department of Earth System Science, University of California, Irvine, California 92602, United States

13 ⁵Center of Air Quality Simulation and System Analysis, Chinese Academy of Environmental Planning,
14 Beijing 100012, China

15 *Correspondence to: Ruili Wu (wurl15@mails.tsinghua.edu.cn)*

16 **Abstract.** This paper presents the first development and evaluation of the reduced-complexity air quality
17 model for China. In this study, a reduced-complexity air quality intervention model over China (InMAP-
18 China) is developed by linking a regional air quality model, a reduced-complexity air quality model, an
19 emission inventory database for China, and a health impact assessment model to rapidly estimate the air
20 quality and health impacts of emission sources in China. The modelling system is applied over mainland
21 China for 2017 under various emission scenarios. A comprehensive model evaluation is conducted by
22 comparison against conventional CMAQ simulations and ground-based observations. We found that
23 InMAP-China satisfactorily predicted total PM_{2.5} concentrations in terms of statistical performance.
24 Compared with the observed PM_{2.5} concentrations, the mean bias (MB), normalized mean bias (NMB),
25 and correlations of the total PM_{2.5} concentrations are -8.1 µg/m³, -18%, and 0.6, respectively. The
26 statistical performance is considered to be satisfactory for a reduced-complexity air quality model and
27 remains consistent with that evaluated in the United States. The underestimation of total PM_{2.5}
28 concentrations was mainly caused by its composition, primary PM_{2.5}. In terms of the ability to quantify
29 source contributions of PM_{2.5} concentrations, InMAP-China presents similar results in comparison with
30 those based on the CMAQ model, the difference is mainly caused by the different treatment of secondary

31 inorganic aerosols in the two models. Focusing on the health impacts, the annual PM_{2.5}-related premature
32 mortality estimated using InMAP-China in 2017 was 1.92 million, which was 25 ten thousand deaths
33 lower than that estimated based on CMAQ simulations as a result of underestimation of PM_{2.5}
34 concentrations. This work presents a version of the reduced-complexity air quality model over China,
35 provides a powerful tool to rapidly assess the air quality and health impacts associated with control policy,
36 and to quantify the source contribution attributable to many emission sources.

37 **1 Introduction**

38 With rapid urbanization and industrialization, fine particulate matter pollution less than 2.5 μm in
39 diameter (PM_{2.5}) has become a major environmental issue in China. High PM_{2.5} concentrations can be
40 observed over eastern China from satellite observations (Xiao et al., 2020) and the PM_{2.5} concentrations
41 have been largely decreased since 2013 due to the effective control measures taken by Chinese
42 governments (Zhao et al., 2021). PM_{2.5} can affect air quality, ecosystems, and climate change and damage
43 human health through short-term or long-term exposure. The Global Burden of Disease study reported
44 that 1.1 million premature deaths were caused by long-term PM_{2.5} exposure over China in 2015 (Cohen
45 et al., 2017).

46 State-of-the-science three-dimensional air quality models (AQMs) have been widely used in China
47 as tools to simulate regional PM_{2.5} concentrations, quantify the contributions to total PM_{2.5} concentrations
48 resulting from emission sources and assess the benefits associated with control measures (Chang et al.;
49 2019, Li et al., 2015; Zhang et al., 2015; Zhang et al., 2019). The Weather Research and Forecasting
50 model-Community Multiscale Air Quality Modelling System (WRF-CMAQ) (Appel et al., 2017; Chang
51 et al., 2019), the Weather Research and Forecasting model coupled with Chemistry (WRF-Chem)
52 (Reddington et al., 2019), the Weather Research and Forecasting model-Comprehensive Air Quality
53 Model Extension (WRF-CAMx) (Li et al., 2015), and the Global Adjoint model of Atmospheric
54 Chemistry (GEOS-Chem Adjoint) (Zhang et al., 2015) were frequently used in previous studies. To
55 conduct a series of simulations for multiple scenarios or quantify the separate contributions attributable
56 to multiple sources, large computational resources and run time are required while utilizing conventional
57 AQMs. To address these challenges and to improve the availability and accessibility of air quality
58 modelling, a number of reduced-complexity models have been developed by the air quality research
59 community. The three representative reduced-complexity air quality models frequently used are the

60 Estimating Air Pollution Social Impacts Using Regression (EASIUR) model (Heo et al., 2016; Heo et
61 al., 2017), the updated Air Pollution Emission Experiments and Policy (APEEP2) model (Muller et al.,
62 2007; Muller et al., 2011) and the Intervention for Air Pollution model (InMAP) (Tessum et al., 2017).
63 A recent study compares three reduced-complexity models, EASIUR, APEEP2, and InMAP, and the
64 results indicate that these three models are consistent in their assessment of the marginal social cost at
65 the county level (Gilmore et al., 2019). Reduced-complexity air quality models are less computationally
66 intensive and easier to use. However, it is not available for China. Therefore, it is essential to develop a
67 reduced-complexity air quality model over China to quickly predict PM_{2.5} concentrations and the
68 associated health impacts of emission sources.

69 The reduced-complexity intervention model for air pollution, InMAP, was developed by Tessum et
70 al. (Tessum et al., 2017) to rapidly assess the air pollution, health, and economic impacts resulting from
71 marginal changes in air pollutant emissions. Compared with conventional air quality models, InMAP has
72 the advantage of time efficient, can predict annual-average PM_{2.5} concentrations within few hours but
73 with a modest reduction in accuracy compared with CTMs. InMAP reduces the running time by
74 simplifying the physical and chemical process. InMAP has been used to assess marginal health damage
75 of location-specific emission sources (Goodkind et al., 2019), to quantify the health impacts of individual
76 coal-fired power plants in the United States (Thind et al., 2019) and to estimate the health benefits of
77 control policies considering specific locations (Sergi et al., 2020). However, to date, a version of the
78 reduced-complexity air quality intervention model over China is absent.

79 In this work, based on the source code of the version 1.6.1 of InMAP model, a reduced-complexity
80 air quality intervention model over China (InMAP-China) is developed to rapidly predict the air quality
81 and estimate the health impacts of emission sources in China. The modelling system is applied over
82 mainland China for 2017 under various emission scenarios to examine model performance. Comparisons
83 against conventional air quality models and surface observations are performed in this study. The model
84 applicability and limitations are also declared.

85 The paper is organized as follows: Section 2.1 presents the components of InMAP-China including
86 the interface development between WRF-CMAQ and InMAP to generate parameters of the base
87 atmospheric state, the preprocessed process of emission input data and the exposure-response functions
88 employed in this model. Section 2.2 introduces the evaluation protocol, including the statistical variables
89 adopted and the simulation design in this study. Section 3 presents the evaluation of InMAP-China's

90 predictions of PM_{2.5} air quality and PM_{2.5}-related health impacts in several simulations. Section 4
91 summarizes the conclusions and limitations of this study.

92 **2 Description of InMAP-China model**

93 **2.1 Model components and configurations**

94 The reduced-complexity intervention model for air pollution, InMAP, was developed by Tessum et
95 al. (Tessum et al., 2017) to rapidly assess the air pollution, health, and economic impacts resulting from
96 marginal changes in air pollutant emissions. The model has been widely used in studies (Sergi et al.,
97 2020; Thind et al., 2019; Goodkind et al., 2019; Dimanchevi et al., 2019) focusing on PM_{2.5} pollution
98 and health, economic impacts resulting from emission sources in the United States. In this model, the
99 continuous equation of atmospheric pollutants is solved at an annual scale, and the run time can be
100 reduced. The parameters used to represent physical and chemical processes for simplified simulation are
101 calculated prior to using CTM output data. PM_{2.5} air quality and PM_{2.5}-related premature mortality are
102 predicted and output in the InMAP model.

103 In this work, a Chinese version of the reduced-complexity air quality intervention model InMAP-
104 China is developed for the purpose of rapidly estimating the PM_{2.5} concentration and associated health
105 impacts of emission sources. Figure 1 shows the model framework. Based on the source code of the
106 InMAP model, three-step development work is conducted to establish InMAP-China. First, we develop
107 a preprocessed interface to calculate physical and chemical process parameters using the WRF-CMAQ
108 output variables to support the simplified simulation in InMAP-China. Second, air pollutant emission
109 data are preprocessed to an appropriate format for the InMAP-China simulation. Third, the exposure-
110 response function of the GEMM model is employed in InMAP-China and replaces the original default
111 function to assess PM_{2.5}-related health impacts.

112 Table 1 presents the basic configurations of InMAP-China. The simulation domain is over East
113 Asia and covers mainland China. The spatial resolution is 36 km. Fourteen vertical layers are used in
114 InMAP-China, ranging from the surface layer to the top level of the tropospheric layer.

115 **2.1.1 Parameter interface development for simplified simulation in InMAP-China**

116 We develop a preprocessed interface to calculate physical and chemical process parameters using
117 WRF-CMAQ output variables for simplified simulation in InMAP-China based on the Environmental
118 Protection Agency's (EPA) work (Baker et al., 2020). The main step of the preprocessed interface

119 includes meteorological and chemical variable extraction and merging, unit conversion, vertical layer
120 mapping, physical and chemical process parameter calculation and average processing. The hourly
121 chemical and meteorological variable outputs from the WRF-CMAQ modelling system are converted
122 into annual-average physical and chemical process parameters required for simplified simulation.

123 A NETCDF file containing the three-dimensional annually averaged parameters to characterize
124 atmospheric advection, dispersion, mixing, chemical reaction, and deposition is generated. Table 2 shows
125 the relationship between the annual-average parameters for simplified simulation and the original hourly
126 variables. In InMAP-China, the annual averaged component and the deviation of wind speed to represent
127 advection are calculated using hourly elements. The offset of wind vectors in different directions may
128 result in some uncertainties in this process. The parameters of eddy diffusion and convective transport
129 are precalculated using hourly elements, including temperature, pressure, boundary layer height, etc. The
130 annual wet deposition rate is determined by the rainwater mixing ratio and cloud fractions. The annual
131 dry deposition rate of particles and gaseous pollutants at the surface level is precalculated using friction
132 speed, heat flux, radiation flux and land cover.

133 The simplification of chemical reactions is different among pollutants. For NO_x , NH_3 , and volatile
134 organic compound (VOC) precursors, the annual averaged gas-particle partitioning is adopted and
135 calculated before using the output concentrations of species from CMAQ. For SO_2 pollutants, the annual
136 oxidation rate of two major conversion pathways for SO_2 is calculated using concentrations of hydroxyl
137 radical (HO) and hydrogen peroxide (H_2O_2) in CMAQ, and the conversion is estimated in InMAP-China.

138 **2.1.2 Prior WRF-CMAQ simulation**

139 To generate the meteorological and chemical parameters required by InMAP-China, a one-year
140 WRF-CMAQ simulation is conducted to output hourly meteorological and chemical-related variables in
141 the year 2017. Tables S1 and S2 show the major configurations of the WRF-CMAQ modelling system.
142 The WRF model is driven by the National Centers for Environmental Prediction Final Analysis (NCEP-
143 FNL) (<https://doi.org/10.5065/D6M043C6>) reanalysis data to provide the initial and boundary conditions.
144 The meteorological fields derived from the WRF model is used to drive the CMAQ model (Appel et al.,
145 2016) simulations. The air pollutant emissions used here include anthropogenic emissions over China
146 derived from the MEIC model (<http://meicmodel.org/>), anthropogenic emissions over the region of East
147 Asia outside China derived from the MIX-2010 inventory (Li et al., 2015), and biogenic emissions
148 derived from the MEGANv2.10 model. The CB05 chemical mechanism and the AERO6 aerosol module
149 are employed in the model simulation.

150 Table S3 summarizes the performance statistics of meteorological variables, including surface
151 temperature, relative humidity, and wind speed, in China in 2017, as simulated by the WRF model. The
152 hourly observed data of major meteorological variables derived from the National Climate Data Center
153 (NCDC) are utilized here. The results show that the meteorological variables simulated by the WRF
154 model agree well with the surface observations, which is consistent with previous studies (Wu et al.,
155 2019; Zheng et al., 2015; Hong et al., 2017). The model performs well on the predictions of surface
156 temperature, with an MB of -0.7 K, an NMB of -6.1%, and R of 0.9. The predictions of relative humidity
157 at a height of 2 metres are relatively satisfied with an MB of 4.1% and an NMB of 6.1%. The predictions
158 of wind speed at a height of 10 metres are slightly overestimated, with an MB of 0.3 m/s and an NMB
159 of 12.4%, which may be caused by out-of-date USGS land use data employed in the model runs.

160 The SO₂, NO₂ and PM_{2.5} concentrations modelled across the domain agree well with the surface
161 observations in terms of the statistical performance and monthly variations. Table S4 summarizes the
162 performance of the statistics of major air pollutant concentrations. The nationwide annual averaged PM_{2.5}
163 concentration simulated in 2017 in China was 42.1 µg/m³. Compared with the observed PM_{2.5} of 45.9
164 µg/m³, there are slight underpredictions with an MB of 3.7 µg/m³ and NMB of 8.1%. The CMAQ model
165 has moderate underpredictions of the NO₂ concentrations and SO₂ concentrations, which may be related
166 to the uncertainties of emission inputs. For modelled NO₂ concentrations, MB and NMB are -4.6 µg/m³
167 and -13.9%, respectively. For modelled SO₂ concentrations, MB and NMB are -0.8 µg/m³ and -4.5%,
168 respectively. Figure S3 shows the monthly variation. The variation trend of the observed SO₂, NO₂, and
169 PM_{2.5} concentrations can basically be reproduced in the CMAQ simulations.

170 **2.1.3 Preprocessed emission input data**

171 Additionally, we develop the preprocessed module to generate vector emission input for the
172 InMAP-China simulation. This module can allocate air pollutant emissions vertically and horizontally to
173 supply the missing parameters for the emission file and convert them into shapefile vector format. The
174 emission data are preprocessed by source and altitude.

175 The anthropogenic emissions of five sectors in China in 2017 from the MEIC inventory
176 (<http://meicmodel.org/>), the anthropogenic emissions over regions outside mainland China in Asia from
177 the MIX-2010 inventory (Li et al., 2015), and the natural emissions estimated using the MEGANv2.10
178 model (Guenther et al., 2012) are employed in this study. Gridded anthropogenic emissions of 0.3
179 degrees for the residential, transportation, and agricultural sectors are preprocessed and input to the
180 surface layer. The gridded air pollutant emissions of the industrial sector and noncoal power plants are

181 preprocessed for allocation to attitudes ranging from 130 metres to 240 metres and 130 metres to 890
182 metres, respectively.

183 The emissions of coal-fired power plants (CPPs) are preprocessed as point sources. The air pollutant
184 emissions and the stack attribution of each unit are provided in the emission file. Because the stack
185 attribution of the power unit is missed in the MEIC inventory, we supplied the information in the
186 preprocessed module based on NEI (National Emission Inventory data) data of power units. For stack
187 height/stack diameter, a linear relationship is first established (see Figure S1), and then, supplementation
188 for these two parameters of Chinese power plants is conducted by using the relationships. The fixed
189 value for the other two variables of stack attribution is set here because the PM_{2.5} concentrations
190 attributable to power plants (CPPs-PM_{2.5}) are less sensitive to the two variables (see Figure S2). The
191 stack gas exit velocity and stack gas exit temperature of the power unit are 6 m/s and 313 K, respectively.

192 The air pollutant emissions over regions outside mainland China in Asia and the natural emissions
193 simulated by MEGANv2.10 are preprocessed and input to the surface layer.

194 **2.1.4 Exposure-response function from GEMM**

195 In InMAP-China, we employ the exposure-response function from GEMM to estimate PM_{2.5}-related
196 premature mortality, which was developed by Burnett et al. (Burnett et al., 2018). Premature mortality
197 due to noncommunicable diseases (NCDs) and lower respiratory infections (LRIs) was considered in this
198 study. Mortality is determined by the mortality incidence rate, population, and attributable fraction (AF)
199 to certain PM_{2.5} concentrations. The national mortality incidence rate and the population data were derived
200 from the GBD2017 study (Institute for Health Metrics and Evaluation). The spatial distribution of the
201 population in 2015 from the Gridded Population of World Version 4 (Doxsey et al., 2015) was employed
202 to allocate the population in 2017.

203 **2.2 Evaluation protocol**

204 **2.2.1 Evaluation method**

205 In this study, the performances of the InMAP-China predictions are evaluated by comparison
206 against CMAQ simulations and surface observations. Model-to-model comparison and model-to-
207 observation comparison have both been used to evaluate the performance of reduced-complexity air
208 quality models in previous studies (Tessum et al., 2017, Gilmore et al., 2019).

209 The following aspects are considered to make an evaluation. First, we examine the ability of
210 InMAP-China to predict PM_{2.5} concentrations at different emission levels, which will be introduced in

211 Section 3.1. Second, to examine the ability to quantify source contributions to PM_{2.5} concentrations, we
212 compare the InMAP-China's predictions of the sectoral contributions attributable to power, industry,
213 residential, transportation, and agriculture with those based on the CMAQ model, which will be
214 presented in Section 3.2. Third, focusing on the health impacts, the PM_{2.5}-related premature mortality
215 predicted by InMAP-China is also compared with mortality estimation based on PM_{2.5} exposure derived
216 from CMAQ, which is presented in Section 3.3.

217 The statistical parameters used in this study include the correlation coefficient (R), mean bias (MB),
218 mean error (ME), normalized mean bias (NMB), normalized mean error (NME), and root mean square
219 error (RMSE). The statistical analyses on the performance of InMAP-China are similar to our previous
220 evaluation of conventional CTMs (Zheng et al., 2015; Wu et al., 2019).

221 The annual averaged observed PM_{2.5} concentrations in 2017 were calculated using hourly
222 concentration data from the China National Environmental Monitoring Center, CNEMC
223 (<http://www.cnemc.cn/>). More than 1400 national monitoring sites for air pollutant concentrations are
224 included in the simulation domain.

225 **2.2.2 Experimental design**

226 We design eleven simulations to examine the model ability of InMAP-China in this study. Table 3
227 shows the sequence of simulations.

228 InMAP_TOT represents the baseline simulation with maximum emissions input, in which five
229 sectoral anthropogenic emissions derived from the MEIC inventory, natural emissions derived from the
230 MEGANv2.10 model, and Asian emissions outside mainland China derived from the MIX-2010
231 inventory are combined as emission inputs. Five sectoral and five abatement simulations are also
232 conducted to examine the ability of InMAP-China to predict concentration changes in response to
233 sectoral emissions and abatement emissions. The emission inputs for these ten simulations have been
234 declared in Table 3. The annual averaged physical and chemical process parameters are calculated based
235 on the output variables of WRF-CMAQ model, which has already been mentioned in Section 2.1.2.
236 Based on the above input, the particle continuity equations are solved by InMAP-China model to obtain
237 the annual averaged PM_{2.5} concentrations at the steady state of atmosphere.

238 In order to make a comparison with the InMAP-China simulations, eleven CMAQ simulations are
239 also performed under the same emission inputs. The hourly PM_{2.5} concentrations simulated by CMAQ
240 in 2017 are averaged at obtain the annual averaged PM_{2.5} concentrations. Due to limited computational

241 resources, each simulation is conducted for four representative months (January, April, July, and October)
242 in 2017.

243 **3 Results and Discussion**

244 **3.1 Model performance of PM_{2.5} concentrations**

245 **3.1.1 Total PM_{2.5} concentrations**

246 Figure 3 shows the performance evaluation of total PM_{2.5} concentrations in the InMAP_TOT
247 simulations. Compared with the observed annual averaged PM_{2.5} concentrations, the total PM_{2.5}
248 concentrations are moderately underpredicted by InMAP-China with an MB of -8.1 μg/m³ and an NMB
249 of -18.1%. Compared with the CMAQ predictions, the total PM_{2.5} concentrations are also underpredicted,
250 with an MB of -5.3 μg/m³ due to the underprediction of primary PM_{2.5}. Consistent air pollutant emissions
251 are employed in the CMAQ and InMAP-China simulations. Therefore, the underpredictions are caused
252 by the different mechanisms in the two models. Basically, InMAP-China reproduces the spatial pattern
253 of total PM_{2.5} concentrations simulated by CMAQ. Notably, significant overpredictions of PM_{2.5}
254 concentrations can be observed over mountain areas across Northern China, and the complex terrain and
255 large emission intensity increase the challenge of predicting PM_{2.5} concentrations using the reduced-
256 complexity air quality model in this region.

257 Figure 4 shows a comparison of PM_{2.5} compositions. Compared with the CMAQ results, the
258 InMAP-China predictions of PM_{2.5} compositions are satisfactory, with NMBs for SO₄²⁻, NO₃⁻, NH₄⁺, and
259 primary PM_{2.5} equal to 13%, -8%, -10%, and -23%, respectively. The predictions of SO₄²⁻, NO₃⁻, and
260 NH₄⁺ perform better than those of primary PM_{2.5}. Figure 5 and Figure 6 compare the spatial distribution
261 of PM_{2.5} compositions, and similar overpredictions of PM_{2.5} compositions can be observed in the
262 mountain area in Northern China.

263 The ability of InMAP-China to predict PM_{2.5} compositions is also examined at various emission
264 levels. Figure 7 compares the concentrations of PM_{2.5} compositions and the proportions of secondary
265 inorganic aerosols (hereafter, SNA) in total PM_{2.5} concentrations in different scenarios by two models.
266 In the InMAP_TOT scenario, the proportion of SNA is 56%, which is extremely close to the 50%
267 proportion in the WRF-CMAQ simulations. In five emission abatement simulations, the proportion was
268 approximately equal to that in the baseline scenario because the linearly treated chemical reaction
269 relationship of SNA was employed in InMAP-China. However, focusing on the simulations of five
270 sectoral emission scenarios, a significant difference can be observed, which is mainly caused by the

271 difference in chemical treatments in InMAP-China and CMAQ. In this situation, the impacts on PM_{2.5}
272 concentrations are distinct due to the nonlinear emission-concentration process.

273 **3.1.2 Marginal change in PM_{2.5} concentrations**

274 Figure 8 compares the InMAP-China and CMAQ predictions of population-weighted PM_{2.5}
275 concentrations and PM_{2.5} compositions for eleven emission scenarios. Marginal changes in air pollutant
276 concentrations are defined as 1 µg/m³ by normalizing the population-weighted air pollutant
277 concentrations of each scenario using the largest value among all scenarios modelled by CMAQ. The
278 InMAP-China reproduces CMAQ predictions on the marginal change in population-weighted PM_{2.5}
279 concentrations, with a NMB of -12% and correlations of 0.98, as shown in Figure 8(a). This performance
280 is similar to that predicted by InMAP in the United States (Tessum et al., 2017).

281 Figure 8(b)-(f) compares the predictions of PM_{2.5} compositions. The InMAP-China predictions of
282 SO₄²⁻, NO₃⁻, NH₄⁺ and primary PM_{2.5} agree well with the CMAQ results, but the predictions of secondary
283 organic aerosol (SOA) are the poorest. The marginal changes in NO₃⁻ and primary PM_{2.5} concentrations
284 are moderately underpredicted by InMAP-China, with NMB values of -13% and -21%, respectively.
285 Conversely, the marginal change in SO₄²⁻ concentrations is overpredicted with an NMB of 23%. The
286 marginal change in NH₄⁺ predicted by InMAP-China agrees well with the CMAQ predictions. Because
287 few reaction pathways of SOA are included in the CB05 mechanism in the CMAQ simulations, SOAs
288 are underpredicted in the entire modelling system.

289 The regional performance of the changes in PM_{2.5} and its compositions for eleven emission
290 scenarios is also examined in this study. Figures S4-S7 show the regional results. Four regions, including
291 the Beijing-Tianjin-Hebei region (BTH), Yangtze River Delta (YRD), Pearl River Delta (PRD), and Fen
292 Wei Plain (FWP), are analysed here (see Figure 2). At the regional level, the CMAQ predicted marginal
293 changes in population-weighted PM_{2.5} concentrations, and its composition can be reproduced by InMAP-
294 China, which is similar to the nationwide performance. However, the marginal change in SO₄²⁻
295 concentrations over the BTH is significantly overpredicted by InMAP-China, with an NMB of 135%,
296 which is expected to be improved by optimizing the representation of the annual sulfate oxidation rate
297 in this region.

298 **3.2 Model performance of source contributions**

299 Figure 9 shows the contribution of each sector to PM_{2.5} concentrations nationwide and at the regional
300 scale, and Table 4 displays the proportion value of sectoral contribution based on two models. The

301 predictions of the source contributions of PM_{2.5} concentrations in InMAP-China are basically reliable
302 compared with those based on the CMAQ model, and the difference can be explained.

303 The results based on the two models indicate that the industrial and residential sectors are the first
304 and second contributors among the five sectors. The contribution of the electricity sector is comparable
305 when using the two models, while the contributions of transportation and agriculture are moderately
306 different, which is mainly due to the difference in the model mechanism and the treatment of secondary
307 inorganic aerosols in the two models. At the regional scale, the difference in the sectoral contribution
308 caused by the mechanism in the two models is more significant than at the national scale.

309 **3.3 Model performance of PM_{2.5}-related premature mortality**

310 Figure 10 compares the predictions of PM_{2.5}-related premature mortality based on two models at
311 the provincial level. The PM_{2.5}-related premature mortality estimated using InMAP-China was 1.92
312 million people in 2017. Compared with the CMAQ-based estimations, 25 ten thousand deaths are under-
313 predicted by InMAP-China because of underestimation of total PM_{2.5} concentrations in the baseline
314 simulation. At the provincial level, the PM_{2.5}-related premature mortality in Beijing city, Tianjin city,
315 Hebei province and Shanghai city is slightly overpredicted by InMAP-China, with the relative difference
316 ranging from 4% to 15%. Conversely, for the other majority of provinces, PM_{2.5}-related premature
317 mortality is under-predicted by InMAP-China, with the relative difference ranging from -3% to -44%.

318 **4 Conclusions**

319 This work develops a reduced-complexity air quality intervention model over China and presents a
320 comprehensive evaluation by comparing CMAQ simulations and surface observations. InMAP-China
321 has the advantage of being time-efficient in conducting air quality predictions and health impact
322 assessments of emission sources in China.

323 InMAP-China performed well for the prediction of PM_{2.5} concentrations. The model satisfactorily
324 predicts total PM_{2.5} concentrations in the baseline simulation in terms of statistical performance.
325 Compared with the observed PM_{2.5} concentrations, the MB, NMB, and correlations of the total PM_{2.5}
326 concentrations are -8.1 μg/m³, -18%, and 0.6, respectively. The statistical performance is satisfactory for
327 a reduced-complexity air quality model and remains consistent with the performance evaluation in the
328 United States. The underestimation of total PM_{2.5} mainly comes from the primary PM_{2.5}. Moreover, the
329 spatial pattern of total PM_{2.5} concentrations can be reproduced in InMAP-China, while an overestimation

330 over the mountain area in Northern China can be observed. The large emission intensity and complex
331 terrain over this region increase the difficulty of modelling concentrations in this area. The predictions
332 of source contributions to $PM_{2.5}$ concentrations by InMAP-China are comparable with those based on
333 the CMAQ model, and the difference is mainly caused by the uncertainty of the simplification of
334 chemical process in the InMAP-China. Focusing on the predictions of health impacts, InMAP-China
335 shows moderate under-predictions of 25 ten thousand people deaths compared with CMAQ-based
336 predictions due to the underestimation of total $PM_{2.5}$ concentrations.

337 Although the modelling system has an acceptable performance, research work is suggested to
338 further improve the model performance. This study is subject to some limitations and uncertainties. In
339 InMAP-China, the annual-average chemical and physical processes parameters are calculated using
340 hourly parameters from WRF-CMAQ. Complicated seasonal and daily variations affecting the formation
341 and transportation of particulate matter are challenging to retain. The intensity of advection of the air
342 mass is supposed to be weakened due to the offset of the wind vector in the averaging process, which
343 was also pointed out in a previous study. Moreover, InMAP-China has difficulty predicting SOA
344 concentrations because reaction pathways for SOA are insufficient in this modelling system.

345 The development of InMAP-China aims at providing an alternative to the conventional CTMs to
346 predicting the $PM_{2.5}$ concentrations due to emission change in the mainland of China. InMAP-China has
347 the advantage of time efficiency and a satisfactory performance in this study; however, this model has a
348 modest reduction in accuracy compared with conventional CTMs; hence, some limitations still exist for
349 model applications. In terms of the applicability of this modelling system, we recommend users to select
350 InMAP-China as a prior tool with the following objectives: quantification of the contribution of multiple
351 emission sources in baseline atmospheric conditions, for instance, the $PM_{2.5}$ air quality and health impacts
352 contributed by dozens of categories of fine emission sources, and rapid estimation of the general air
353 quality and health benefits attributable to a series of control policies. Instead, if the objective of
354 simulations is to predict the actual situation and pre-estimate the reductions in $PM_{2.5}$ concentrations due
355 to control measures, conventional CTMs are a better choice because the change in atmospheric
356 conditions along with emission change should be taken into account.

357

358 **Code and data availability**

359 The source code for the localized version of reduced-complexity air quality model over China (InMAP-
360 China), which is developed based on the original InMAP model over the United states. The data related
361 to this study as well as the user manual are available at <https://doi.org/10.5281/zenodo.5111961>.

362 **Author contributions**

363 RL. Wu and Q. Zhang designed the research and RL. Wu carried them out. RL. Wu, CW. Tessum and
364 Y. Zhang contributed to model development. RL. Wu prepared the manuscript with contributions from
365 all co-authors.

366 **Competing interests**

367 The authors declare no competing interests.

368 **Acknowledgements**

369 This work was supported by the National Natural Science Foundation of China (41921005 and
370 41625020). And this work was also funded under Assistance Agreement No. RD835871 awarded by the
371 U.S. EPA to Yale University. The views expressed in this manuscript are those of the authors alone and
372 do not necessarily reflect the views and policies of the U.S. EPA. The EPA does not endorse any products
373 or commercial services mentioned in this publication.

374

375

376

377

378

379

380

381

382 **References**

- 383 A. Xiu, J. E. Pleim. Development of a Land Surface Model. Part I: Application in a Mesoscale
384 Meteorological Model. *Journal of Applied Meteorology*, 40:192-209, 2011.
- 385 Appel, K.W., Napelenok, S.L., Hogrefe, C., Foley, K.M., Pouliot, G.A., Murphy, B., Heath, N., Roselle,
386 S., Pleim, J., Bash, J.O., Pye, H.O.T., Mathur, R. Overview and evaluation of the Community Multiscale
387 Air Quality (CMAQ) modelling system version 5.2. *Air Pollution Modelling and its Application XXV*,
388 11:63-72. ITM 2016. Springer Proceedings in Complexity. Springer, Cham, doi: 10.1007/978-3-319-
389 57645-9_11, 2017.
- 390 Appel, K.W., Napelenok, S.L., Hogrefe, C., Foley, K.M., Pouliot, G.A., Murphy, B., Heath, N., Roselle,
391 S., Pleim, J., Bash, J.O., Pye, H.O.T., Mathur, R. Overview and evaluation of the Community Multiscale
392 Air Quality (CMAQ) modelling system version 5.2. *Air Pollution Modelling and its Application XXV*,
393 11:63-72. ITM 2016. Springer Proceedings in Complexity. Springer, Cham, doi: 10.1007/978-3-319-
394 57645-9_11, 2017.
- 395 Baker, K. R.; Amend, M.; Penn, S.; Bankert, J.; Simon, H.; Chan, E.; Fann, N.; Zawacki, M.; Davidson,
396 K.; Roman, H., A database for evaluating the InMAP, APEEP, and EASIUR reduced complexity air-
397 quality modelling tools. *Data in Brief*, 28, 2020.
- 398 Burnett, R.; Chen, H.; Szyszkowicz, M.; Fann, N.; Hubbell, B.; Pope, C. A.; Apte, J. S.; Brauer, M.;
399 Cohen, A.; Weichenthal, S.; Coggins, J.; Di, Q.; Brunekreef, B.; Frostad, J.; Lim, S. S.; Kan, H. D.;
400 Walker, K. D.; Thurston, G. D.; Hayes, R. B.; Lim, C. C.; Turner, M. C.; Jerrett, M.; Krewski, D.; Gapstur,
401 S. M.; Diver, W. R.; Ostro, B.; Goldberg, D.; Crouse, D. L.; Martin, R. V.; Peters, P.; Pinault, L.;
402 Tjepkema, M.; Donkelaar, A.; Villeneuve, P. J.; Miller, A. B.; Yin, P.; Zhou, M. G.; Wang, L. J.; Janssen,
403 N. A. H.; Marra, M.; Atkinson, R. W.; Tsang, H.; Thach, Q.; Cannon, J. B.; Allen, R. T.; Hart, J. E.;
404 Laden, F.; Cesaroni, G.; Forastiere, F.; Weinmayr, G.; Jaensch, A.; Nagel, G.; Concin, H.; Spadaro, J.
405 V., Global estimates of mortality associated with long-term exposure to outdoor fine particulate matter.
406 *Proceedings of the National Academy of Sciences of the United States of America*, 115, (38), 9592-9597,
407 2018.
- 408 C. J. Walcek, Taylor GR. A Theoretical Method for Computing Vertical Distributions of Acidity and
409 Sulfate Production within Cumulus Clouds. *Journal of the Atmospheric Science*, 43:339-55, 1986.

410 Chang, X.; Wang, S.; Zhao, B.; Xing, J.; Liu, X.; Wei, L.; Song, Y.; Wu, W.; Cai, S.; Zheng, H.; Ding,
411 D.; Zheng, M., Contributions of inter-city and regional transport to PM_{2.5} concentrations in the Beijing-
412 Tianjin-Hebei region and its implications on regional joint air pollution control. *Science of the Total*
413 *Environment*, 660, 1191-1200, 2019.

414 Cohen, A. J.; Brauer, M.; Burnett, R.; Anderson, H. R.; Frostad, J.; Estep, K.; Balakrishnan, K.;
415 Brunekreef, B.; Dandona, L.; Dandona, R.; Feigin, V.; Freedman, G.; Hubbell, B.; Jobling, A.; Kan, H.;
416 Knibbs, L.; Liu, Y.; Martin, R.; Morawska, L.; Pope, C. A., III; Shin, H.; Straif, K.; Shaddick, G.; Thomas,
417 M.; van Dingenen, R.; van Donkelaar, A.; Vos, T.; Murray, C. J. L.; Forouzanfar, M. H., Estimates and
418 25-year trends of the global burden of disease attributable to ambient air pollution: an analysis of data
419 from the Global Burden of Diseases Study 2015. *Lancet* 389, (10082), 1907-1918, 2017.

420 Dimanchevi, E. G.; Paltsev, S.; Yuan, M.; Rothenberg, D.; Tessum, C. W.; Marshall, J. D.; Selin, N. E.,
421 Health co-benefits of sub-national renewable energy policy in the US. *Environmental Research Letters*,
422 14, (8) ,2019.

423 Doxsey-Whitfield E, MacManus K, Adamo S B, Susana B, Pistolesi L, Squires J, Borkovska O and
424 Baptista S R Taking advantage of the improved availability of census data: a first look at the gridded
425 population of the world, version 4. *Papers in Applied Geography*. 1 226–34, 2015.

426 E. J. Mlawer, S. J. Taubman, P. D. Brown, M. J. Iacono, S. A. Clough. Radiative transfer for
427 inhomogeneous atmospheres: RRTM, a validated correlated-k model for the longwave. *Journal of*
428 *Geophysical Research*, 102:16663-82, 1997.

429 Fountoukis C and Nenes A. ISORROPIA II: A Computationally Efficient Aerosol Thermodynamic
430 Equilibrium Model for K⁺, Ca²⁺, Mg²⁺, NH₄⁺, Na⁺, SO₄²⁻, NO₃⁻, Cl⁻, H₂O Aerosols, *Atmospheric*
431 *Chemistry Physics*, 7, 4639-4659, 2007.

432 Gilmore, E. A.; Heo, J.; Muller, N. Z.; Tessum, C. W.; Hill, J. D.; Marshall, J. D.; Adams, P. J., An inter-
433 comparison of the social costs of air quality from reduced-complexity models. *Environmental Research*
434 *Letters*, 14, (7), 2019.

435 Global Burden of Disease Collaborative Network. *Global Burden of Disease Study 2017 (GBD 2017)*
436 *Population Estimates 1950-2017*. Seattle, United States: Institute for Health Metrics and Evaluation
437 (IHME), 2018.

438 Global Burden of Disease Collaborative Network. Global Burden of Disease Study 2017 (GBD 2017)
439 Cause-Specific Mortality 1980-2017. Seattle, United States: Institute for Health Metrics and Evaluation
440 (IHME), 2018.

441 Goodkind AL, Tessum CW, Coggins JS, Hill JD, Marshall JD. Fine-scale damage estimates of particulate
442 matter air pollution reveal opportunities for location-specific mitigation of emissions. Proceedings of the
443 National Academy of Sciences. Apr 3:201816102. <https://doi.org/10.1073/pnas.1816102116>, 2019.

444 Guenther, A. B.; Jiang, X.; Heald, C. L.; Sakulyanontvittaya, T.; Duhl, T.; Emmons, L. K.; Wang, X.,
445 The Model of Emissions of Gases and Aerosols from Nature version 2.1 (MEGAN2.1): an extended and
446 updated framework for modelling biogenic emissions. Geoscientific Model Development Discussions,
447 5, (2), 1503-1560, 2012.

448 Heo, J.; Adams, P. J.; Gao, H. O., Public health costs accounting of inorganic PM_{2.5} pollution in
449 metropolitan areas of the United States using a risk-based source-receptor model. Environment
450 International, 106, 119-126, 2017.

451 Heo, J.; Adams, P. J.; Gao, H. O., Reduced-form modelling of public health impacts of inorganic PM_{2.5}
452 and precursor emissions. Atmospheric Environment, 137, 80-89, 2016.

453 Hong, C.; Zhang, Q.; Zhang, Y.; Tang, Y.; Tong, D.; He, K., Multi-year downscaling application of two-
454 way coupled WRF v3.4 and CMAQ v5.0.2 over east Asia for regional climate and air quality modelling:
455 model evaluation and aerosol direct effects. Geoscientific Model Development, 10, (6), 2447-2470, 2017.

456 J. E. Pleim. A Combined Local and Nonlocal Closure Model for the Atmospheric Boundary Layer. Part
457 I: Model Description and Testing. Journal of Applied Meteorology and Climatology, 46:1383-95, 2007.

458 J. S. Chang, R. A. Brost, I. S. A. Isaksen, S. Madronich, P. Middleton, W. R. Stockwell, et al. A three-
459 dimensional Eulerian acid deposition model: Physical concepts and formulation. Journal of Geophysical
460 Research, 92:14681-700, 1987.

461 J. S. Kain. The Kain–Fritsch Convective Parameterization: An Update. Journal of Applied Meteorology.
462 2004, 43:170-81.

463 Li, M.; Zhang, Q.; Kurokawa, J.-i.; Woo, J.-H.; He, K.; Lu, Z.; Ohara, T.; Song, Y.; Streets, D. G.;
464 Carmichael, G. R.; Cheng, Y.; Hong, C.; Huo, H.; Jiang, X.; Kang, S.; Liu, F.; Su, H.; Zheng, B., MIX:
465 a mosaic Asian anthropogenic emission inventory under the international collaboration framework of the

466 MICS-Asia and HTAP. *Atmospheric Chemistry and Physics*, 17, (2), 935-963, 2017.

467 Li, X.; Zhang, Q.; Zhang, Y.; Zheng, B.; Wang, K.; Chen, Y.; Wallington, T. J.; Han, W.; Shen, W.; Zhang,
468 X.; He, K., Source contributions of urban PM_{2.5} in the Beijing-Tianjin-Hebei region: Changes between
469 2006 and 2013 and relative impacts of emissions and meteorology. *Atmospheric Environment*, 123, 229-
470 239, 2015.

471 Liu, F.; Zhang, Q.; Tong, D.; Zheng, B.; Li, M.; Huo, H.; He, K. B., High-resolution inventory of
472 technologies, activities, and emissions of coal-fired power plants in China from 1990 to 2010.
473 *Atmospheric Chemistry and Physics*, 15, (23), 13299-13317, 2015.

474 M.-D. Chou, M. J. Suarez, C.-H. Ho, M. M.-H. Yan, K.-T. Lee. Parameterizations for Cloud Overlapping
475 and Shortwave Single-Scattering Properties for Use in General Circulation and Cloud Ensemble Models.
476 *Journal of Climate*, 11:202-14, 1998.

477 Muller, N. Z., Mendelsohn, R. Measuring the damages of air pollution in the United States. *Journal of*
478 *Environmental Economics and Management*, 54(1), 1–14. <https://doi.org/10.1016/j.jeem.2006.12.002>,

479 Muller, N. Z., Mendelsohn, R., & Nordhaus, W. Environmental accounting for pollution in the United
480 States economy. *American Economic Review*, 101(5), 1649-75. DOI:10.1257/aer.101.5.1649, 2011.

481 Multi-resolution Emission Inventory of China (<http://meicmodel.org/>).

482 National Centers for Environmental Prediction/National Weather Service/NOAA/US Department of
483 Commerce NCEP FNL Operational Model Global Tropospheric Analyses, continuing from July 1999
484 Dataset (<https://doi.org/10.5065/D6M043C6>), 2000.

485 Reddington, C. L.; Conibear, L.; Knote, C.; Silver, B.; Li, Y. J.; Chan, C. K.; Arnold, S. R.; Spracklen,
486 D. V., Exploring the impacts of anthropogenic emission sectors on PM_{2.5} and human health in South and
487 East Asia. *Atmospheric Chemistry and Physics*, 19, (18), 11887-11910, 2019.

488 Sergi, B. J.; Adams, P. J.; Muller, N. Z.; Robinson, A. L.; Davis, S. J.; Marshall, J. D.; Azevedo, I. L.,
489 Optimizing Emissions Reductions from the U.S. Power Sector for Climate and Health Benefits.
490 *Environmental science & technology*, 54, (12), 7513-7523, 2020.

491 Skamarock W, Klemp J, Dudhia J, Gill D, Barker D, Duda M, Huang X, Wang Wand Powers J A
492 description of the Advanced Research WRF Version 3 NCAR technical note (Boulder, CO: National
493 Center for Atmospheric Research), 2008.

494 Tessum, C. W.; Hill, J. D.; Marshall, J. D., InMAP: A model for air pollution interventions. *PLoS One*,
495 12, (4), e0176131, 2017.

496 Thind, M. P. S.; Tessum, C. W.; Azevedo, I. L.; Marshall, J. D., Fine Particulate Air Pollution from
497 Electricity Generation in the US: Health Impacts by Race, Income, and Geography. *Environmental*
498 *Science & Technology*, 53, (23), 14010-14019, 2019.

499 United States Environmental Protection Agency. National Emission Inventory data.
500 <https://www.epa.gov/air-emissions-inventories/2011-national-emissions-inventory-nei-data>. 2011.

501 Whitten G Z, Heo G, Kimura Y, et al. A new condensed toluene mechanism for Carbon Bond CB05-TU.
502 *Atmospheric Environment*, 44(40SI):5346-5355, 2010.

503 Wu, R.; Liu, F.; Tong, D.; Zheng, Y.; Lei, Y.; Hong, C.; Li, M.; Liu, J.; Zheng, B.; Bo, Y.; Chen, X.; Li,
504 X.; Zhang, Q., Air quality and health benefits of China's emission control policies on coal-fired power
505 plants during 2005–2020. *Environmental Research Letters*, 14, (9), 094016, 2019.

506 Xiao, Q. Y.; Geng, G. N.; Liang, F. C.; Wang, X.; Lv, Z.; Lei, Y.; Huang, X. M.; Zhang, Q.; Liu, Y.; He,
507 K., Changes in spatial patterns of PM_{2.5} pollution in China 2000–2018: Impact of clean air policies.
508 *Environment international*, 141, 105776, 2020.

509 Zhang, L.; Liu, L. C.; Zhao, Y. H.; Gong, S. L.; Zhang, X. Y.; Henze, D. K.; Capps, S. L.; Fu, T. M.;
510 Zhang, Q.; Wang, Y. X., Source attribution of particulate matter pollution over North China with the
511 adjoint method. *Environmental Research Letters*, 10, (8), 2015.

512 Zhang, Q.; Zheng, Y.; Tong, D.; Shao, M.; Wang, S.; Zhang, Y.; Xu, X.; Wang, J.; He, H.; Liu, W.; Ding,
513 Y.; Lei, Y.; Li, J.; Wang, Z.; Zhang, X.; Wang, Y.; Cheng, J.; Liu, Y.; Shi, Q.; Yan, L.; Geng, G.; Hong,
514 C.; Li, M.; Liu, F.; Zheng, B.; Cao, J.; Ding, A.; Gao, J.; Fu, Q.; Huo, J.; Liu, B.; Liu, Z.; Yang, F.; He,
515 K.; Hao, J., Drivers of improved PM_{2.5} air quality in China from 2013 to 2017. *Proceedings of the*
516 *National Academy of Sciences of the United States of America*, 116, (49), 24463-24469, 2019.

517 Zheng, B.; Zhang, Q.; Zhang, Y.; He, K. B.; Wang, K.; Zheng, G. J.; Duan, F. K.; Ma, Y. L.; Kimoto, T.,
518 Heterogeneous chemistry: a mechanism missing in current models to explain secondary inorganic aerosol
519 formation during the January 2013 haze episode in North China. *Atmospheric Chemistry and Physics*,
520 15, (4), 2031-2049, 2015.

521

522 **Table 1. Model configurations in InMAP-China.**

Category	Parameters	Configurations
Basic	Research area and period	China, 2017
	Spatial resolution	36 km × 36 km
	Vertical layers	14 layers
	Run type	Steady run
	Variable grid	Static grid
	Projection	Lambert
	Grid numbers	305816
	Meteorological and chemical parameters	Calculated using variables from WRFv3.8-CMAQv5.2
Input	Anthropogenic emissions	MEIC, MIX, MEGAN
	Population data	GPW 2015 and GBD 2017
	Baseline mortality rate	GBD 2017
Output	Air pollutants	PM _{2.5} and its composition concentrations
	Mortality	PM _{2.5} -related premature mortality

523

524

525

526

527

528

529

530

531

532

Table 2 The relationship between parameters for simplified simulation and original variables.

WRF-CMAQ's Variables	Descriptions	InMAP-China's Parameters	Descriptions
U, V, W	Wind fields	UAvg, UDeviation VAvg, VDeviation WAvg, WDeviation	Advection and mixing coefficients
PH, PHB	Base state of geopotential and perturbation geopotential	Dz	Layer heights
PBLH	Planetary boundary layer height	M2d, M2u, Kxxyy, Kzz	Mixing coefficients
T	Potential Temperature	SO ₂ Oxidation, PlumeHeight	Chemical reaction rates and plume rise
P, PB	Base state pressure plus perturbation pressure		Chemical reaction rates and plume rise
QRAIN	Mixing ratio of rain	ParticleWetdep, GasWetdep	Wet deposition
QCLOUD	Cloud mixing ratio	SO ₂ Oxidation	Aqueous-phase chemical reaction rates
CLDFRA	Fraction of grid cell covered by clouds	ParticleWetdep, GasWetdep	Wet deposition
SWDOWN, GLW	Downward shortwave and longwave radiative flux at ground level	GasDrydep, ParticleWetdep	Dry deposition
HFX	Surface heat flux	M2d, M2u, Kxxyy, Kzz, Drydep	Mixing and dry deposition
UST	Friction velocity		Mixing and dry deposition
LU_INDEX	Land use type	M2d, M2u, Kxxyy, Kzz	Mixing
DENS	Inverse air density		Mixing and convert between mixing ratio and mass concentration
aVOC	Anthropogenic VOCs that are SOA precursors	aOrgPartitioning	VOCs/SOA partitioning
aSOA	Anthropogenic SOA		
OH, H ₂ O ₂	Hydroxyl radical and hydrogen peroxide concentrations	SO ₂ Oxidation	Oxidation rates
pNO	ANO ₃ I, ANO ₃ J	NOPartitioning	

gNO	NO and NO ₂		NO _x /pNO ₃ partitioning
pNH	ANH ₄ I, ANH ₄ J	NHPartitioning	NH ₃ /pNH ₄
gNH	NH ₃		partitioning

534

535

536

537

538

539

540

541

542

543

544

545

546

547

548

549

550

551

552

553

554

555

556

557

558 **Table 3 Simulation experiments conducted using InMAP-China.**

Class	Simulations	Emission input	Physical and chemical parameter input
Sec1	InMAP_POW	Power plants emissions	
Sec2	InMAP_INDUS	Industrial emissions	
Sec3	InMAP_TRANS	Transportation emissions	
Sec4	InMAP_RESI	Residential emissions	
Sec5	InMAP_AGRI	Agricultural emissions	
BASE	InMAP_TOT	Five sectoral anthropogenic emissions and natural emissions	
Aba1	InMAP_RE10	Reduce the air pollutants emissions by 10% based on InMAP_TOT emissions	
Aba2	InMAP_RE30	Reduce the air pollutants emissions by 30% based on InMAP_TOT emissions	
Aba3	InMAP_RE50	Reduce the air pollutants emissions by 50% based on InMAP_TOT emissions	Converted using WRF-CMAQv5.2 simulation data in the year of 2017;
Aba4	InMAP_RE70	Reduce the air pollutants emissions by 70% based on InMAP_TOT emissions	Remain the same in all simulations.
Aba5	InMAP_RE90	Reduce the air pollutants emissions by 90% based on InMAP_TOT emissions	

559

560

561

562

563

564

565

566

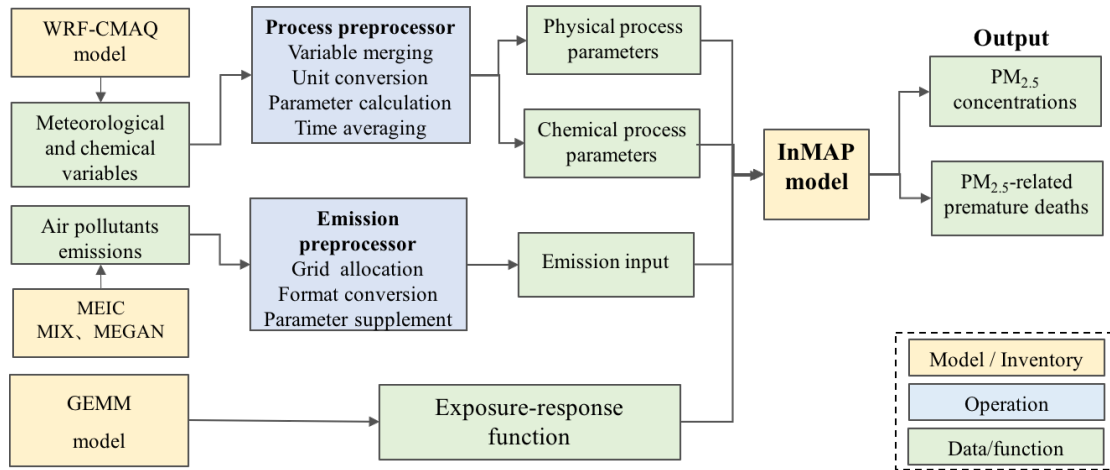
567

568 **Table 4 Comparison of the proportions of sectoral contributions to PM_{2.5} concentrations using InMAP-**
 569 **China and CMAQ.**

Sector	National		BTH		YRD		PRD		FWPY	
	CMAQ	InMAP- P- China	CMAQ	InMAP- P- China	CMAQ	InMAP- P- China	CMAQ	InMAP- P- China	InMAP- P- China	
Power	6.9%	8.1%	6.2%	9.4%	7.4%	8.6%	10.4%	8.2%	7.0%	10.0%
Industry	30.8%	35.0%	30.2%	38.2%	33.3%	39.1%	37.5%	35.4%	27.7%	31.9%
Residential	25.9%	28.1%	24.7%	28.2%	17.9%	20.8%	19.5%	28.4%	30.0%	33.8%
Transportation	14.0%	17.3%	13.4%	15.6%	15.7%	21.2%	17.1%	17.5%	13.2%	15.0%
Agriculture	22.5%	11.5%	25.5%	10.4%	25.7%	12.4%	15.4%	11.6%	22.0%	9.4%

570
 571
 572
 573
 574
 575
 576
 577
 578
 579
 580
 581
 582

InMAP-China model



583

584

Figure 1 Model framework of InMAP-China.

585

586

587

588

589

590

591

592

593

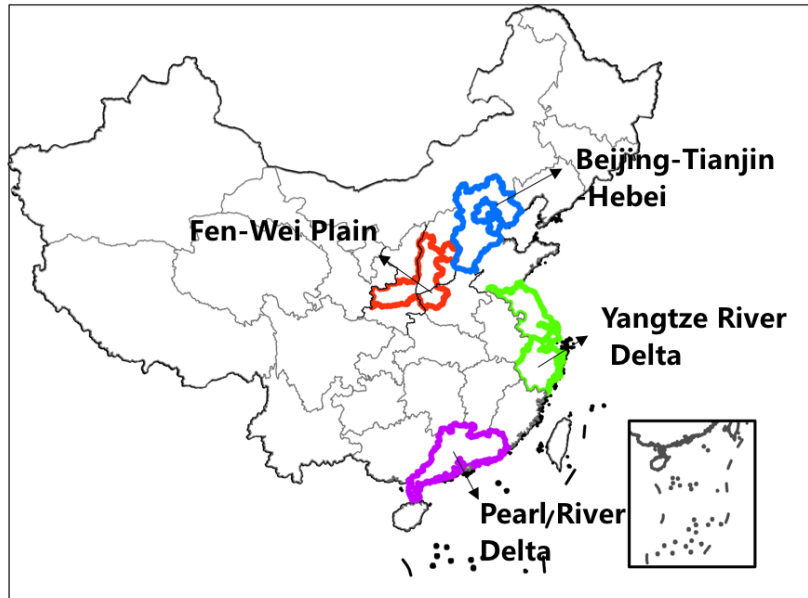
594

595

596

597

598



599

600

601

Figure 2 Four key regions defined in this study, including the Beijing-Tianjin-Hebei region, Yangtze River Delta region, Pearl River Delta region and Fen Wei Plain region.

602

603

604

605

606

607

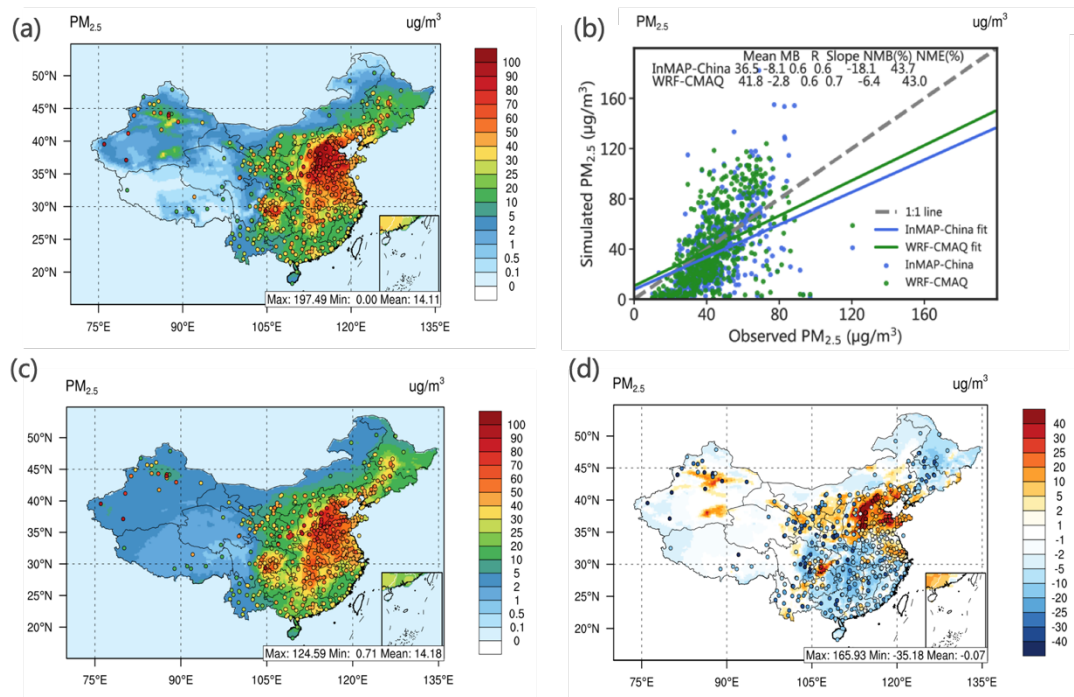
608

609

610

611

612



613

614 **Figure 3 The spatial pattern and statistical metrics of total PM_{2.5} concentrations predicted by InMAP-China**

615 **and WRF-CMAQ.** Panels (a) and (c) display the spatial patterns of total PM_{2.5} concentrations predicted by InMAP-

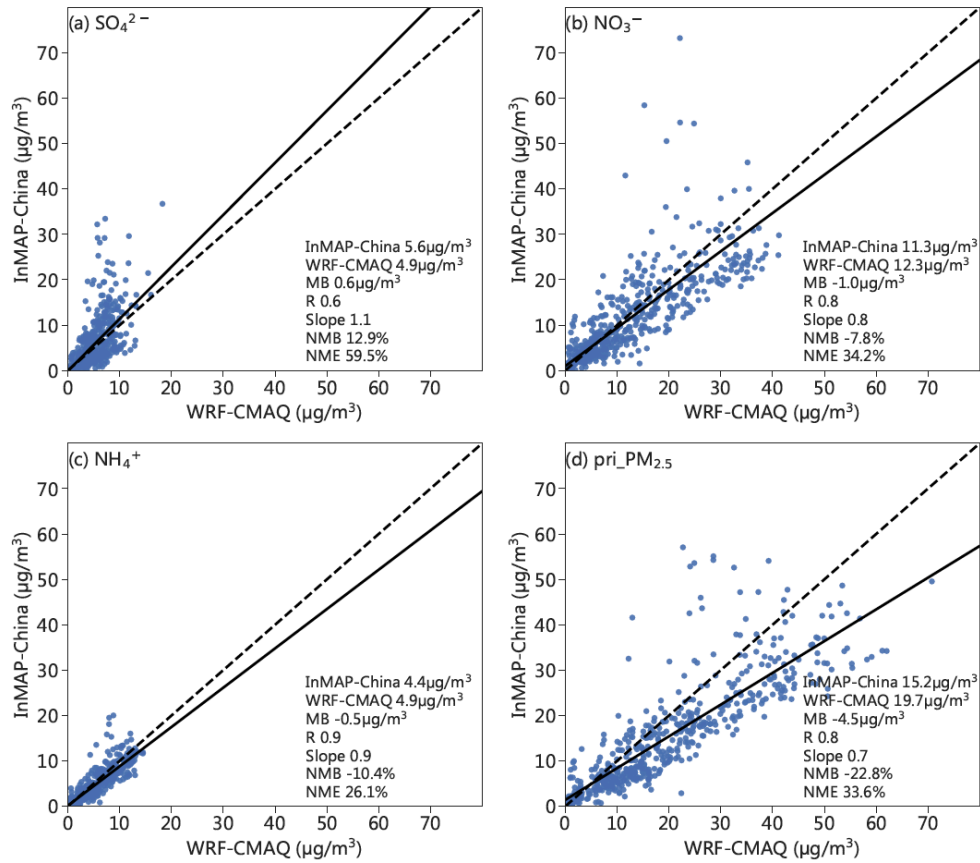
616 China and WRF-CMAQ, respectively. Panel (d) presents the difference in the spatial distribution of the total PM_{2.5}

617 concentrations predicted by the two models. Panel (b) shows the statistical metrics between the simulated and

618 observed PM_{2.5}. The observed total PM_{2.5} concentrations are marked as circles in panel (a) and panel (c). In panel

619 (d), the circle shows the difference between the PM_{2.5} simulated by InMAP-China and the observed PM_{2.5}. The same

620 colorbar is utilized in the contour and the marked circle.

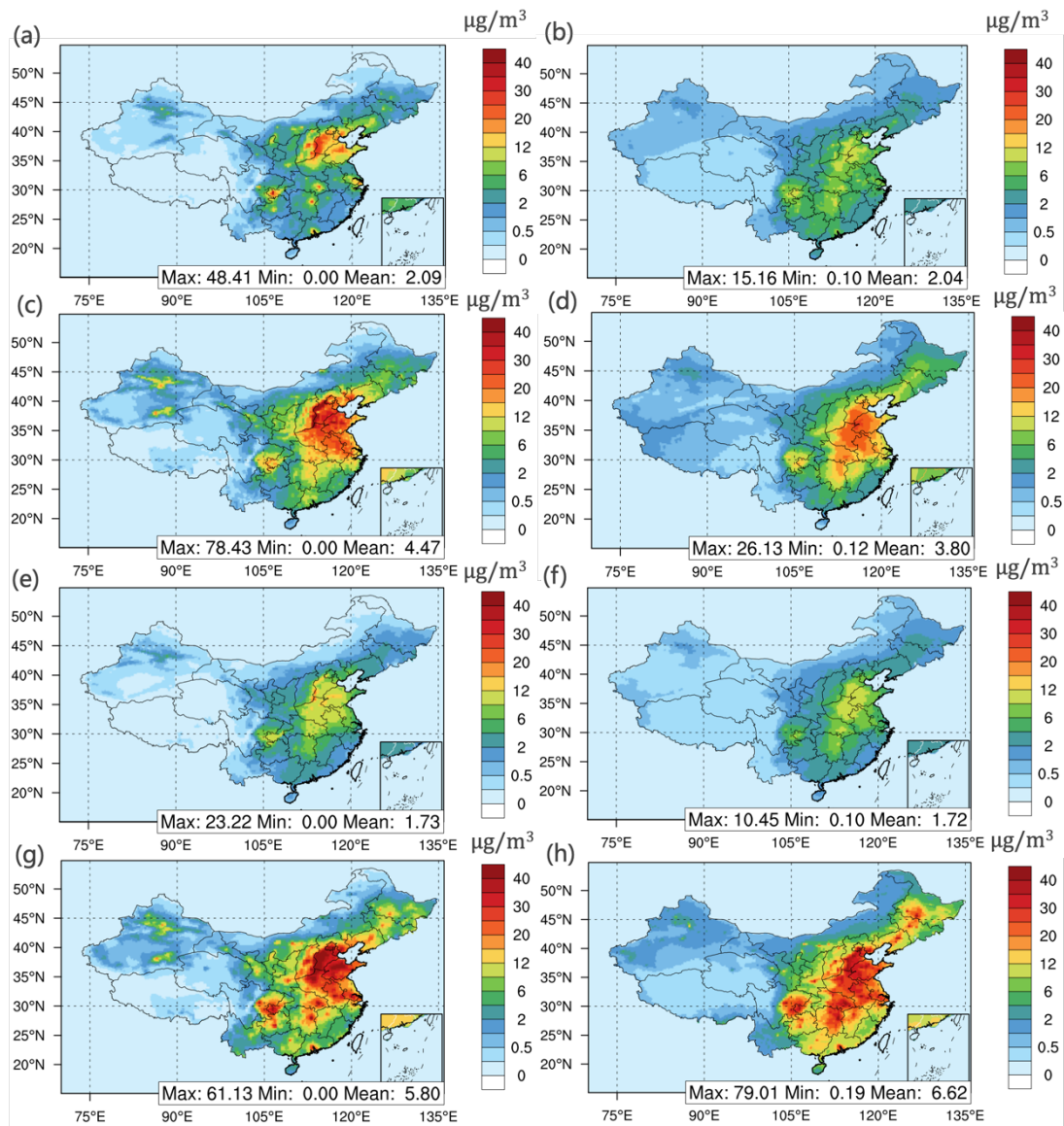


621

622 **Figure 4 Scatter plot comparing the PM_{2.5} composition concentration modelled by the InMAP-China and**

623 **WRF-CMAQ models. Panels (a), (b), (c) and (d) display sulfate, nitrate, ammonium, and primary PM_{2.5},**

624 **respectively. The statistical metrics are labelled in the lower right corner in each panel.**



625

626

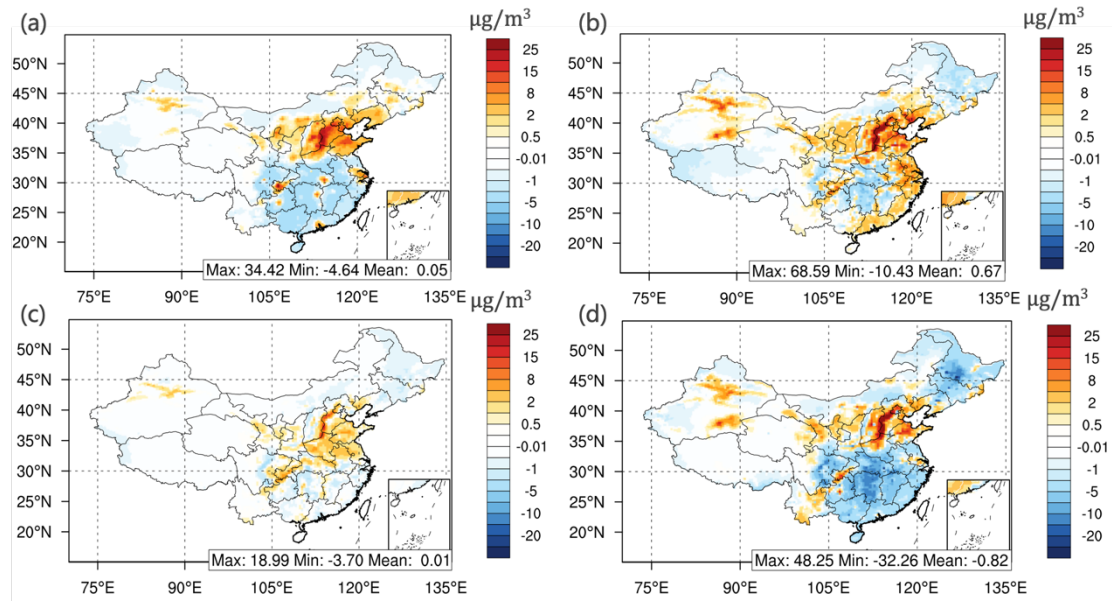
Figure 5 The spatial pattern of PM_{2.5} compositions modelled by the InMAP-China and WRF-CMAQ models.

627

Panels (a), (c), (e), and (g) present the sulfate, nitrate, ammonium, and primary PM_{2.5}, respectively, simulated by

628

InMAP-China in the InMAP-TOT scenario. Panels (b), (d), (f), and (h) present the results modelled by WRF-CMAQ.



629

630

Figure 6 The difference in the spatial pattern of $PM_{2.5}$ compositions between InMAP-China and WRF-CMAQ.

631

Panels (a), (b), (c), and (d) display sulfate, nitrate, ammonium, and primary $PM_{2.5}$, respectively.

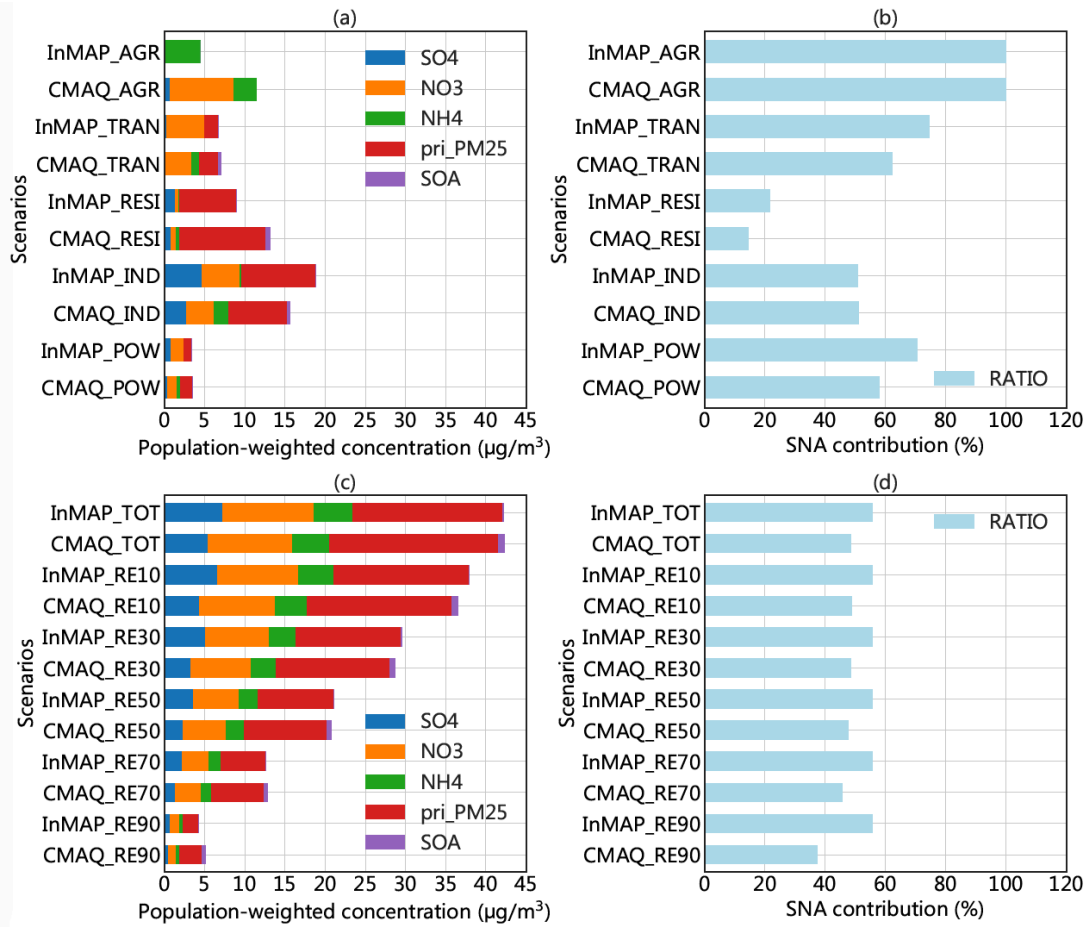
632

633

634

635

636



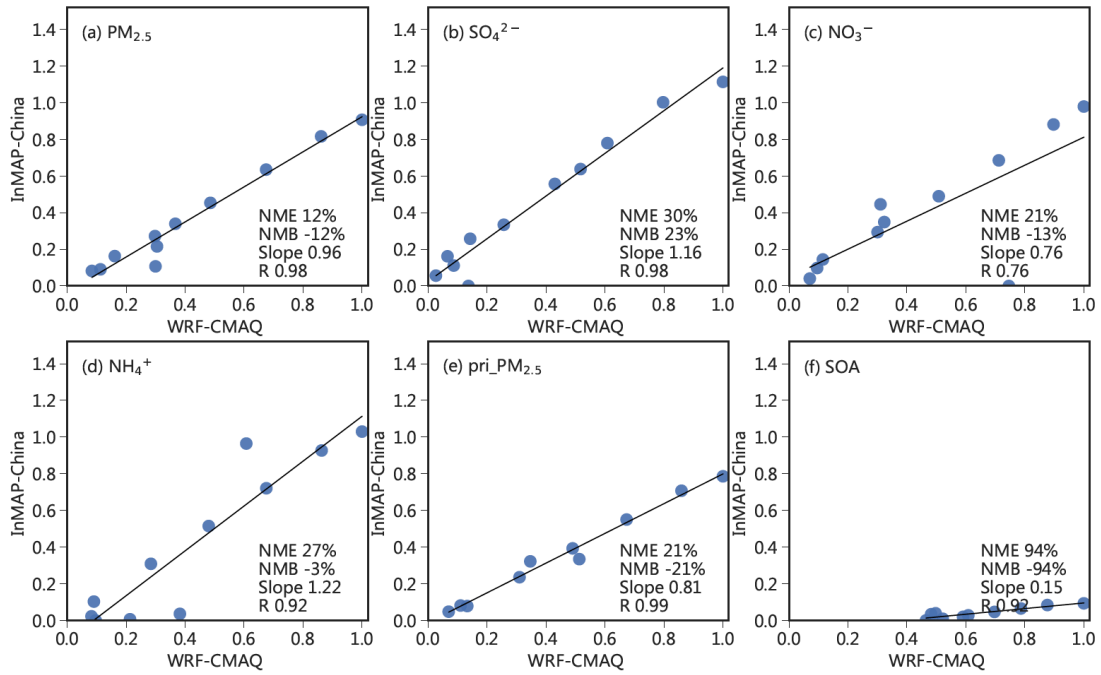
637

638 **Figure 7 Comparison of PM_{2.5} component concentrations and SNA contributions in these eleven simulations.**

639 (a) and (c) show the modelled PM_{2.5} compositions. Panel (a) presents the results of sectoral emission scenarios, and

640 panel (c) presents the results of the baseline and emission abatement scenarios. Panels (b) and (d) present the SNA

641 contribution (%) for each scenario.



642

643

Figure 8 Marginal change in nationwide annual average population-weighted $PM_{2.5}$ concentration and its

644

composition as modelled by InMAP-China and WRF-CMAQ for eleven emissions scenarios. The population-

645

weighted pollutant concentration for each scenario is normalized using the largest value among all scenarios

646

modelled by CMAQ. The eleven dots represent the eleven scenarios, and the statistical metrics are labelled in the

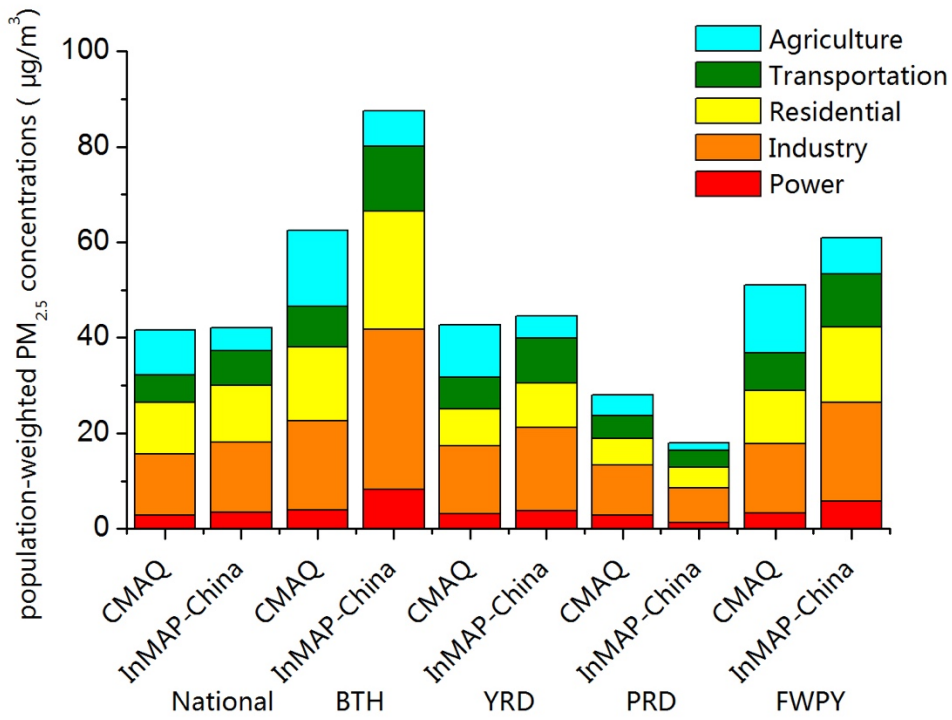
647

lower right corner for each panel.

648

649

650



651

652 **Figure 9 Comparison of source contributions to population-weighted PM_{2.5} concentrations estimated by the**
 653 **two models.**

654

655

656

657

658

659

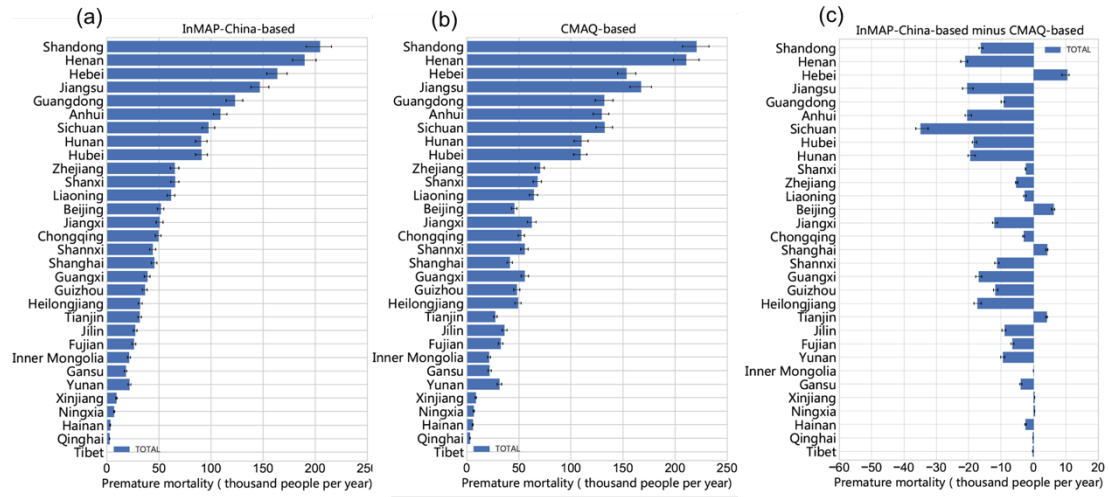
660

661

662

663

664



665

666 **Figure 10 Comparison of PM_{2.5}-related premature mortality based on two models. (a) InMAP-China-based;**

667 **(b) CMAQ-based; and (c) difference between the two models.**

668

669

670

671

672

673

674

675

676

677

678

679

680

681

682

683